

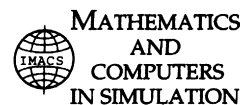


ELSEVIER

Available online at www.sciencedirect.com



Mathematics and Computers in Simulation xxx (2011) xxx–xxx



www.elsevier.com/locate/matcom

Suppression of Rayleigh–Taylor instability using electric fields

Lyudmyla L. Barannyk^{a,*}, Demetrios T. Papageorgiou^b, Peter G. Petropoulos^c

^a Department of Mathematics, University of Idaho, P.O. Box 441103, Brink Hall 317, Moscow, ID 83844, United States

^b Department of Mathematics, Imperial College London, United Kingdom

^c Department of Mathematical Sciences, New Jersey Institute of Technology, United States

Received 29 November 2009; received in revised form 14 June 2010; accepted 29 November 2010

Abstract

This study considers the stability of two stratified immiscible incompressible fluids in a horizontal channel of infinite extent. Of particular interest is the case with the heavier fluid initially lying above the lighter fluid, so that the system is susceptible to the classical Rayleigh–Taylor instability. An electric field acting in the horizontal direction is imposed on the system and it is shown that it can act to completely suppress Rayleigh–Taylor instabilities and produces a dispersive regularization in the model. Dispersion relations are derived and a class of nonlinear traveling waves (periodic and solitary) is computed. Numerical solutions of the initial value problem of the system of model evolution equations that demonstrate a stabilization of Rayleigh–Taylor instability due to the electric field are presented.

© 2010 IMACS. Published by Elsevier B.V. All rights reserved.

Keywords: Rayleigh–Taylor instability; Electric fields; Traveling waves; Solitary waves

1. Introduction

Electric fields acting parallel to an interface separating two immiscible fluids of different material properties, have been shown to induce a dispersive effect (Melcher and Schwarz [8], Tilley et al. [10], Papageorgiou and Vanden-Broeck [9]). Such effects on Rayleigh–Taylor (R–T) instabilities have not been studied systematically. Further more in inviscid R–T flows, a finite-time singularity is encountered (Baker et al. [1]) and the effect of electric field regularization is an interesting physical mechanism that can affect such phenomena. In the related problem of liquid sheet rupture, it has been shown by Tilley et al. [10] that rupture singularities can be delayed or completely suppressed by sufficiently strong electric fields. Such a paradigm is investigated here for the R–T problem. In the case of background shear, Kelvin–Helmholtz (K–H) instabilities are present and produce larger short-wave growth rates as compared to R–T instability. The effect of horizontal electric fields on K–H flows has been considered by Grandison et al. [5,6], who studied nonlinear model equations as well as numerical traveling wave solutions of the two-dimensional Euler equations, when the field is strong enough so as to provide a stabilization in conjunction with surface tension. Fields which act perpendicularly to the undisturbed interface, on the other hand, are unstable at least for the regimes of perfect conductors or perfect dielectric fluids. For example, a vertical field can destabilize a (stably stratified) viscous fluid layer wetting the top surface of a horizontal substrate, and cause asymptotic thinning of the layer – Tseluiko and Papageorgiou [13]

* Corresponding author. Tel.: +1 208 885 6719; fax: +1 208 885 5843.

E-mail address: barannyk@uidaho.edu (L.L. Barannyk).

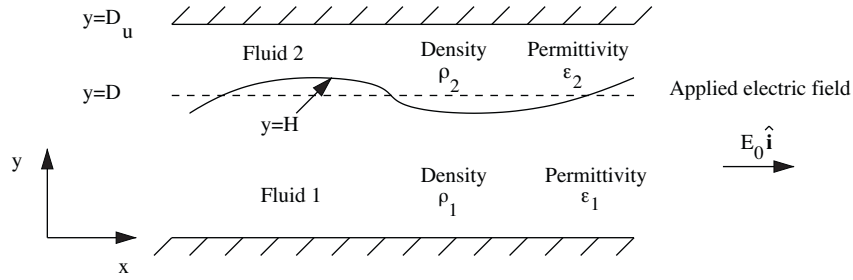


Fig. 1. Schematic of the problem.

(for inclined substrates see Tseluiko and Papageorgiou [11,12]). Also of interest is the study of Gleeson et al. [4], who present a novel electrohydrodynamics derivation of the Benjamin–Ono Kortweg–de Vries equation.

The paper is organized as follows: Section 2 introduces the governing equations and boundary conditions. Section 3 considers the linear stability problem and gives the dispersion relation, while Section 4 derives asymptotically a system of nonlinear evolution equations valid for thin upper layers. Section 5 constructs and computes traveling wave solutions of these equations, with finite as well as infinite wavelengths (solitary waves in the latter case). Section 6 addresses numerically the initial value problems of the system of model evolution equations.

2. Mathematical model

Two immiscible, inviscid, irrotational and incompressible fluids with densities ρ_1, ρ_2 are bound together in an infinite horizontal channel of depth D_u and separated by an interface given by $y = H(x, t)$ in a Cartesian coordinate system, where t is time – see the schematic in Fig. 1. The fluids are assumed to be perfect dielectrics with electrical permittivities ϵ_1 and ϵ_2 and the surface tension coefficient between them is σ . The lower fluid occupies region 1 given by $0 < y < H(x, t)$ and the upper fluid is in region 2 given by $H(x, t) < y < D_u$. A uniform horizontal electric field $\mathbf{E}_0 = (V_0/D)\hat{\mathbf{i}}$ acts, with V_0 the characteristic voltage drop and D is the undisturbed depth of the lower layer. Gravity acts in the negative y -direction with acceleration g . The hydrodynamics are governed by Euler's equations which can be represented in terms of harmonic fluid potentials ϕ_1 and ϕ_2 , say, with the fluid velocity fields given by $\mathbf{u}_{1,2} = \nabla\phi_{1,2}$. The electrostatics derives from the electrostatic limit of Maxwell's equations. Briefly, since the induced magnetic fields are negligible, Faraday's law reads $\nabla \times \mathbf{E}_{1,2} = 0$ where $\mathbf{E}_{1,2}$ is the electric field in each region, and hence we can introduce voltage potentials $V_{1,2}$ such that $\mathbf{E}_{1,2} = -\nabla V_{1,2}$. In addition, since there are no volumetric charge concentrations in the fluids, Gauss's law becomes $\nabla \cdot (\epsilon_{1,2}\mathbf{E}_{1,2}) = 0$, which combined with Faraday's law implies that V_1 and V_2 are also harmonic functions. The field equations are, then

$$\Delta\phi_{1,2} = 0, \quad \Delta V_{1,2} = 0, \quad (1)$$

where $\Delta \equiv (\partial/\partial x^2) + (\partial/\partial y^2)$. The boundary conditions at $y = H(x, t)$ are the kinematic conditions, continuity of normal stresses, continuity of the normal component of the displacement field $\epsilon\mathbf{E}$ and continuity of the tangential component of the electric field:

$$H_t + \phi_{1x}H_x - \phi_{1y} = 0, \quad H_t + \phi_{2x}H_x - \phi_{2y} = 0, \quad (2)$$

$$[\mathbf{n} \cdot \mathbf{T} \cdot \mathbf{n}]_2^1 = \sigma \nabla \cdot \mathbf{n}, \quad (3)$$

$$[\epsilon\mathbf{E} \cdot \mathbf{n}]_2^1 = 0, \quad \mathbf{n} \times [\mathbf{E}]_2^1 = 0, \quad (4)$$

where $[\cdot]_2^1$ denotes the jump in the quantity as the interface is crossed from the lower to the upper fluid, $\mathbf{n} = (-H_x, 1)/(1 + H_x^2)^{1/2}$, $\mathbf{t} = (1, H_x)/(1 + H_x^2)^{1/2}$ are the unit normal (pointing out of region 1) and tangent to the interface, respectively. The stress tensor \mathbf{T} is given by

$$T_{ij} = -p\delta_{ij} + \mathcal{E}_{ij}, \quad \mathcal{E}_{ij} = \epsilon \left(E_i E_j - \frac{1}{2} |\mathbf{E}|^2 \delta_{ij} \right). \quad (5)$$

The first term in T_{ij} is the inviscid hydrodynamic contribution and the second term represents the Maxwell stresses – Jackson ([7], Chap. 6). The analysis proceeds by integrating the Euler equations to obtain a Bernoulli equation at $y = H(x, t)$. The pressure jump across the interface is then eliminated using (3) to yield a nonlinear dynamic interfacial boundary condition given by (11) in dimensionless form. Finally, the boundary conditions on the channel walls are a no penetration condition for the hydrodynamics and no vertical component of the electric field for the electrostatics:

$$\phi_{1y} = V_{1y} = 0 \quad \text{at } y = 0, \quad \phi_{2y} = V_{2y} = 0 \quad \text{at } y = D_u. \quad (6)$$

Horizontally far away from any interfacial disturbances, the electric field tends to its unperturbed value so that

$$V_{jx} \rightarrow E_0|x|, \quad \text{as } |x| \rightarrow \infty, \quad j = 1, 2. \quad (7)$$

Variables are made dimensionless by scaling lengths by D , fluid potentials by $D(gD)^{1/2}$, time by $(D/g)^{1/2}$ and voltages by V_0 (these scalings have been chosen so as to retain gravitational effects in the model and to be able to switch surface tension and electric field effects on or off directly). In what follows we use the same symbols as before for dimensionless quantities. The following dimensionless groups emerge

$$\rho = \frac{\rho_2}{\rho_1}, \quad \epsilon_p = \frac{\epsilon_2}{\epsilon_1}, \quad E_b = \frac{\epsilon_1 V_0^2}{\rho_1 g D^3}, \quad W_e = \frac{\sigma}{\rho_1 g D^2}, \quad H_0 = \frac{D_u}{D}, \quad (8)$$

which represent the density and permittivity ratios, an electric Weber number E_b measuring the strength of the electric field, a Weber number W_e based on the velocity $(gD)^{1/2}$ which is the ratio of surface tension forces to gravitational forces (this is also an inverse Bond number), and the dimensionless channel height H_0 . In terms of dimensionless variables, Eqs. (1) and boundary conditions (2) and (6) remain unaltered; Eqs. (4) become

$$V_{1x}H_x - V_{1y} = \epsilon_p (V_{2x}H_x - V_{2y}) \quad \text{at } y = H(x, t), \quad (9)$$

$$V_{1x} + V_{1y}H_x = V_{2x} + V_{2y}H_x \quad \text{at } y = H(x, t). \quad (10)$$

Finally, a Bernoulli equation at $y = H(x, t)$ is derived as follows. The x - and y -momentum equations of the Euler equations are written in terms of the fluid potential $\phi_{1,2}$ in each respective region, are integrated with respect to x and y , respectively, and evaluated at the interface in order to obtain an expression for the pressure jump across the interface in terms of $\phi_{1,2}$ and their derivatives (the integrals resulting from the x and y integrations are ultimately identical). The Bernoulli equation emerges by eliminating the pressure jump through the use of the normal stress balance (3), which now brings in electric, surface tension and gravitational effects (for more details see Grandison et al. [5]). The resulting equation is

$$\begin{aligned} \phi_{1t} + \frac{1}{2}(\phi_{1x})^2 + \frac{1}{2}(\phi_{1y})^2 - \rho \left(\phi_{2t} + \frac{1}{2}(\phi_{2x})^2 + \frac{1}{2}(\phi_{2y})^2 \right) - (\rho - 1)H &= W_e \frac{H_{xx}}{(1 + H_x^2)^{3/2}} \\ - \frac{E_b}{2}(V_{1x}^2 - V_{1y}^2) \frac{H_x^2 - 1}{1 + H_x^2} + \frac{\epsilon_p E_b}{2}(V_{2x}^2 - V_{2y}^2) \frac{H_x^2 - 1}{1 + H_x^2} + 2E_b \frac{H_x}{1 + H_x^2} V_{1x} V_{1y} \\ - 2\epsilon_p E_b \frac{H_x}{1 + H_x^2} V_{2x} V_{2y} + \bar{K}_p, \end{aligned} \quad (11)$$

where the constant of integration $\bar{K}_p = -(\rho - 1) - \frac{E_b}{2}(1 - \epsilon_p)$ has been determined by evaluating (11) using the undeformed steady-state $H = 1$, $V_{1,2} = x$, $\phi_{1,2} = 0$. It can be seen from (11) that the electric field or surface tension can be removed by selecting E_b or W_e to vanish.

The nonlinear moving boundary problem formulated in this section presents a formidable analytical and computational task and we proceed to explore some of its mathematical and physical properties.

3. Linear stability analysis

Flat interface quiescent flows are exact solutions of the mathematical model given above. We write these stationary states as

$$\mathbf{u}_{1,2} = \mathbf{0}, \quad H = 1, \quad V_{1,2} = x. \quad (12)$$

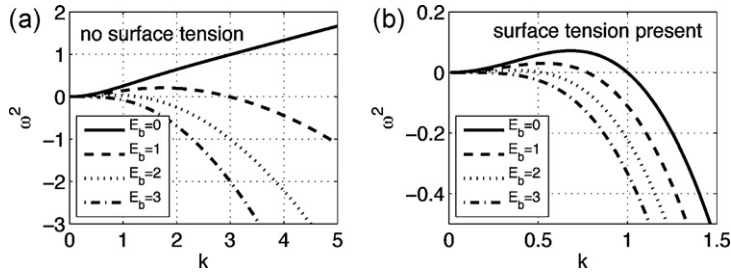


Fig. 2. The dispersion relation as E_b varies (values shown); other parameters are $\rho=2$, $\epsilon_p=2$, $H_0=2$. (a) $W_e=0$, no surface tension. (b) Surface tension present, $W_e=1$.

To study the stability of this state we write $\mathbf{u}_{1,2} = \delta \tilde{\mathbf{u}}_{1,2}$, $H(x, t) = 1 + \delta \tilde{H}(x, t)$, and $V_{1,2} = x + \delta \tilde{V}_{1,2}$, where δ is infinitesimal, and linearize the boundary conditions in the usual way evaluating all tilde variables at the undisturbed level $y=1$. We introduce normal mode solutions:

$$\tilde{\phi}_{1,2} = \hat{\phi}_{1,2}(y)e^{ikx+\omega t}, \quad \tilde{V}_{1,2} = \hat{V}_{1,2}(y)e^{ikx+\omega t}, \quad \tilde{H}(x, t) = \hat{H}e^{ikx+\omega t}, \quad (13)$$

where it is understood that the real part is to be taken. Substitution of (13), after solving for $\hat{\phi}_{1,2}$, $\hat{V}_{1,2}$ in terms of exponential functions, into the linearized kinematic, Bernoulli and electric field boundary conditions at the undisturbed level $y=1$, along with the boundary conditions on walls $y=0$ and $y=H_0$, yields five homogeneous equations for constants of integration involved in $\hat{\phi}_{1,2}$, $\hat{V}_{1,2}$ and the constant \hat{H} . The condition for non-trivial solutions leads to the following dispersion relation:

$$\frac{\omega^2}{k} \left(\coth k - \rho \frac{\cosh k - \tanh(kH_0) \sinh k}{\sinh k - \tanh(kH_0) \cosh k} \right) - (\rho - 1) = -W_e k^2 + \frac{\bar{E}_b k [\cosh k - \tanh(kH_0) \sinh k]}{-(1 - \epsilon_p) \sinh k - \epsilon_p \tanh(kH_0) \cosh k + \tanh(kH_0) (\sinh^2 k / \cosh k)} \quad (14)$$

where $\bar{E}_b = (1 - \epsilon_p)^2 E_b$. The first term on the right hand side of (14) represents surface tension and the second term electric field effects. In the absence of both, it is clear that real positive values of ω are possible if $\rho > 1$, and hence the flow is unstable as expected. The dispersion relation (14) extends that in Papageorgiou and Vanden-Broeck [9] by adding gravity and density stratification to their problem as well as a bounded upper layer. In fact, if we let $H_0 \rightarrow \infty$, set $\rho=0$ and remove gravity by eliminating the term with $(\rho - 1)$, equation (14) reduces to

$$\omega^2 = -W_e k^3 \tanh k - E_b (1 - \epsilon_p)^2 k^2 \frac{\tanh k}{\tanh k + \epsilon_p}, \quad (15)$$

in complete agreement with Papageorgiou and Vanden-Broeck [9].

To observe the stabilizing effect of the electric field it is useful to analyze (14) in the short-wave limit, $k \gg 1$. It can be shown that (we use the fact that $H_0 > 1$ here)

$$\omega^2 = \frac{(\rho - 1)}{(\rho + 1)} k - W_e \frac{k^3}{(\rho + 1)} - \frac{E_b (1 - \epsilon_p)^2}{(\rho + 1)(1 + \epsilon_p)} k^2, \quad k \gg 1. \quad (16)$$

If $\rho < 1$ the system is stable to short waves but when $\rho > 1$ (heavy fluid on top) a short-wave R–T instability follows. Surface tension regularizes this instability as seen from the $-W_e k^3/(\rho + 1)$ term in (14). If surface tension is absent ($W_e=0$), (16) shows that the electric field is capable of stabilizing short waves; this is a novel physical regularization of R–T instability and is found in K–H (see Grandison et al. [6]). A sufficiently large electric field can stabilize R–T instability for all wavenumbers and evidence for this comes from the long wave limit ($k \ll 1$) of (14)- this is not included here but numerical results are given. Fig. 2 summarizes these findings; in panel (a) we take zero surface tension, $W_e=0$, and $\rho=2$, $\epsilon_p=2$ and $H_0=2$, and plot the variation of ω^2 with k as \bar{E}_b increases from zero. It can be seen that the band of unstable waves decreases with increasing \bar{E}_b and in fact disappears completely when \bar{E}_b is larger than 3.0, approximately. When surface tension is included ($W_e=1$) the stability is enhanced as seen from the results in panel (b) of Fig. 2.

Analogous results are found for other values of H_0 as well and in particular H_0 near unity. Writing $H_0 = 1 + \epsilon$ where $0 < \epsilon \ll 1$, we can analyze (14) asymptotically in ϵ to find

$$\omega^2 \rho = (\rho - 1)k^2 - W_e k^4 - \bar{E}_b k^3 \coth k, \quad (17)$$

along with its long-wave version ($k \ll 1$)

$$\omega^2 \rho = (\rho - 1)k^2 - W_e k^4 - \bar{E}_b k^2. \quad (18)$$

The dispersion relations (17) and (18) suggest that a system of model dispersive evolution equations is possible if \bar{E}_b is sufficiently large (non-local and local ones, respectively). Next, we sketch the derivation of such models and construct nonlinear traveling wave solutions of the local model as well as study the dynamics of the local model by solving initial value problems on periodic domains.

4. Evolution equations for thin upper layers

Given a dimensionless undisturbed upper layer thickness ϵ , we look for interfacial waves whose amplitude scales with ϵ but have order one wavelengths, i.e. the waves are long with respect to the upper layer thickness but of comparable length with the lower layer thickness. We separate vertical scales by introducing a new upper layer variable ζ given by

$$y = 1 + \epsilon - \epsilon \zeta. \quad (19)$$

The disturbed interface is given by $H(x, t) = 1 + \epsilon S(x, t)$ with $S(x, t)$ to be found ($\zeta = 0$ on the upper wall and $\zeta = 1 - S(x, t)$ at the interface). Time is scaled according to $\tau = \epsilon^{1/2} t$ —this comes from a balance of unsteadiness and nonlinearity in the Bernoulli equation. The relevant expansions for the fluid and voltage potentials are

$$\phi_1 = \epsilon^{1/2}(\phi_1^{(0)} + \epsilon^2 \phi_1^{(2)} + \dots), \quad \phi_2 = \epsilon^{1/2}(\phi_2^{(0)} + \epsilon^2 \phi_2^{(2)} + \dots), \quad (20)$$

$$V_1 = x + \epsilon V_1^{(1)} + \dots, \quad V_2 = x + \epsilon V_2^{(1)} + \dots \quad (21)$$

where the x terms in (21) represent the background voltage potentials. The solution in the film simplifies due to the fact that $\Delta \equiv (\partial^2 / \partial x^2) + (1/\epsilon^2)(\partial^2 / \partial \zeta^2)$; we find $\phi_2^{(0)} = B(x, \tau)$ and $\phi_2^{(2)} = -\zeta^2 / (2B_{xx})$, where $B(x, \tau)$ is to be determined. The second kinematic condition (2) yields

$$S_\tau + ((S - 1)B_x)_x = 0. \quad (22)$$

The solution of $\Delta V_2 = 0$ subject to the boundary condition $V_{2y} = 0$ at $y = H_0$ gives, to leading order, $V_2^{(1)} = C(x, \tau)$ with $C(x, t)$ to be determined. The problem for $\phi_1^{(0)}$ becomes $\Delta \phi_1^{(0)} = 0$ subject to $\phi_{1y}^{(0)}(x, 1, \tau) = \phi_{1y}^{(0)}(x, 0, \tau) = 0$ (this condition comes from continuity of normal components of velocity, $\nabla \phi_1 \cdot \mathbf{n} = \nabla \phi_2 \cdot \mathbf{n}$ at the interface); the solution is $\phi_1^{(0)} \equiv \text{const.}$, and this simplifies the Bernoulli equation significantly. The Maxwell stresses in the Bernoulli equation (11) can be expressed, to leading order in ϵ , in terms of region 2 potentials alone, i.e. $C(x, \tau)$, by using the electric field boundary conditions (9) and (10) yielding

$$(1 - \epsilon_p)S_x = V_{1y}^{(1)}, \quad V_{1x}^{(1)} = V_{2x}^{(1)} \quad \text{at} \quad \zeta = 1 - S(x, \tau). \quad (23)$$

The Bernoulli equation becomes, to leading order:

$$-\rho \left(\phi_{2\tau}^{(0)} + \frac{1}{2}(\phi_{2x}^{(0)})^2 \right) - (\rho - 1)S = W_e S_{xx} + E_b(1 - \epsilon_p)C_{xx}. \quad (24)$$

It remains to calculate $C(x, \tau)$ in terms of $S(x, t)$. The harmonic problem for $V_1^{(1)}$ has boundary conditions $V_{1y}^{(1)}(x, 0, \tau) = 0$ and $V_{1y}^{(1)}(x, 1, \tau) = (1 - \epsilon_p)S_x$ (along with periodicity in x), and is readily solved in Fourier space to obtain $\hat{V}_1^{(1)} = (i(1 - \epsilon_p)\hat{S} / \sinh k) \cosh ky$, with hats denoting the usual Fourier transform operator. Using the second of conditions (23) immediately yields

$$\hat{C} = i(1 - \epsilon_p)(\coth k) \hat{S}. \quad (25)$$

Introducing new variables

$$\eta(x, \tau) = 1 - S(x, \tau), \quad u(x, \tau) = B_x(x, \tau), \quad (26)$$

representing the scaled upper layer thickness and the horizontal velocity at the interface, respectively, casts the model system into

$$\eta_\tau + (\eta u)_x = 0, \quad (27)$$

$$\rho(u_\tau + uu_x) - (\rho - 1)\eta_x = W_e \eta_{xxx} - E_b(1 - \epsilon_p)C_{xx}, \quad (28)$$

$$\hat{C} = -i(1 - \epsilon_p)(\coth k)\hat{\eta}. \quad (29)$$

The model (27)–(29) is non-local but in the long wave limit ($k \ll 1$) it localizes to

$$\eta_\tau + (\eta u)_x = 0 \quad (30)$$

$$\rho(u_\tau + uu_x) + \beta \eta_x = W_e \eta_{xxx} \quad (31)$$

where $\beta = E_b(1 - \epsilon_p)^2 - (\rho - 1)$. Note that ρ can be removed from the first term of (31) through the transformation $u \rightarrow u/\sqrt{\rho}$ and $\partial/\partial\tau \rightarrow (1/\sqrt{\rho})\partial/\partial\tau$, and this is used in some of the numerical work that follows.

Note that when there is no electric field the model equations, both non-local and local, reduce to shallow water equations in the presence of surface tension.

5. Traveling waves

Looking for solutions of (30) and (31) in the form $\eta = \eta(x - c\tau)$, $u = u(x - c\tau)$ and defining $\xi = x - c\tau$, yields

$$-c\eta' + (\eta u)' = 0 \quad (32)$$

$$\rho(-cu' + \frac{1}{2}(u^2)') + \beta\eta' = W_e\eta''', \quad (33)$$

where primes denote ξ -derivatives. This system can be integrated twice to yield the single nonlinear ODE

$$W_e \left(\frac{d\eta}{d\xi} \right)^2 = \frac{\beta\eta^3 - (\rho c^2 + B)\eta^2 - D\eta - \rho A^2}{\eta} \equiv f(\eta), \quad (34)$$

where A, B and D are constants of integration. Existence of spatially periodic traveling waves hinges on the construction of periodic profiles of (34). Some physical restrictions are that the range of η must satisfy $0 < \eta < 1$ and $\beta > 0$ even if $\rho > 1$. Zeros of the polynomial $P_3(\eta) = \beta\eta^3 - (\rho c^2 + B)\eta^2 - D\eta - \rho A^2$ correspond to local maxima or minima of $\eta(\xi)$ and we require two successive real roots in $0 < \eta < 1$ between which $P_3(\eta)$ is positive; since $\beta > 0$, the three admissible real roots can be ordered as $0 < \eta_1 < \eta_2 \leq \eta_3$ with $\eta_2 < 1$. Then, η_1 and η_2 are the wave trough and crest, respectively, and we can implicitly obtain the profile from the quadrature:

$$\int_{\eta_1}^{\eta} \frac{d\tilde{\eta}}{\sqrt{f(\tilde{\eta})}} = \xi. \quad (35)$$

It is easy to show that even though $f(\eta_1) = f(\eta_2) = 0$, the integral (35) is not singular – in fact, $1/\sqrt{f} \sim 1/(\eta - \eta_1)^{1/2}$ with a similar behavior at η_2 , and the singularities are integrable. The wavelength L is

$$L = 2 \int_{\eta_1}^{\eta_2} \frac{d\eta}{\sqrt{f(\eta)}} = \frac{2}{\sqrt{\beta}} \int_{\eta_1}^{\eta_2} \sqrt{\frac{\eta}{(\eta - \eta_1)(\eta_2 - \eta)(\eta_3 - \eta)}} d\eta = \frac{4\eta_1}{\sqrt{\beta\eta_2(\eta_3 - \eta_1)}} \Pi(\alpha^2, k), \quad (36)$$

where $\alpha^2 = (\eta_2 - \eta_1)/\eta_2$, $k^2 = \eta_3/(\eta_3 - \eta_1)\alpha^2$ and $\Pi(\alpha^2, k)$ is the complete elliptic integral of the third kind. We note that η_1, η_2, η_3 can be found in closed form using the results documented in Bronshtein et al. [2], for example. When $\eta_3 = \eta_2 < 1$, the length tends to infinity and a solitary wave emerges. This can also be seen from (35) because the root η_2 is now repeated. Writing $f(\eta) = (\beta/\eta)(\eta - \eta_1)(\eta - \eta_2)^2$ implies that the conditions $2\eta_2 + \eta_1 = (\rho c^2 + B)/\beta$, $\eta_2^2 + 2\eta_1\eta_2 = -(D/\beta)$ and $\eta_1\eta_2^2 = (\rho A^2/\beta)$ must be satisfied, and the constants A, B, c, D must be chosen so that the constraint $0 < \eta_1 < \eta_2 < 1$ holds. Therefore, it is easy to show using elementary methods that we can have waves of finite periods as well as solitary ones, depending on the parameters. In Fig. 3 we give solutions from two such typical cases; the figure

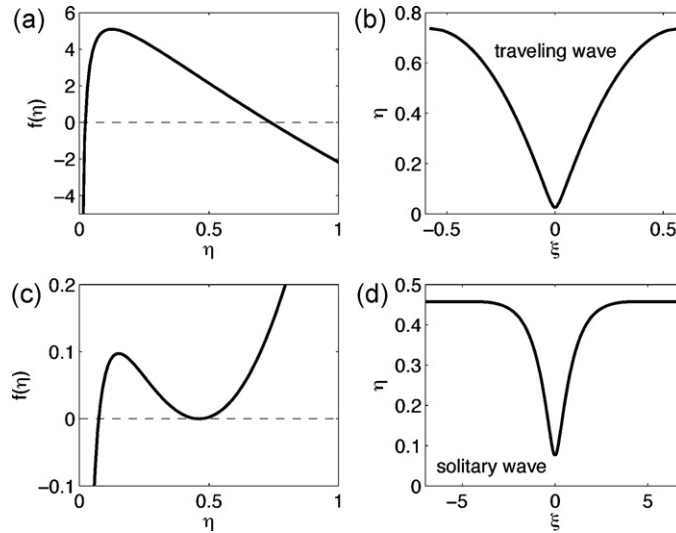


Fig. 3. The function $f(\eta)$ and the corresponding traveling waves: (a) and (b) $W_e = 1$, $\beta = \rho = 2$, $c = 1$, $A = 3/10$, $B = 10$, $D = -8$, leading to periodic traveling waves. (c) and (d) $W_e = 1$, $\beta = 2$, $\rho = 2$, $c = 1$, $A = 0.1268$, $B = 0$, $D = -17/30$ leading to solitary waves.

includes the variation of $f(\eta)$ and the corresponding traveling wave solution $\eta(\xi)$ computed using (35). Panels (a) and (b) correspond to periodic waves and the parameter values are $W_e = 1$, $\beta = \rho = 2$, $c = 1$, $A = 3/10$, $B = 10$, $D = -8$. Panels (c) and (d) correspond to solitary waves with parameters $W_e = 1$, $\beta = 2$, $\rho = 2$, $c = 1$, $A = 0.1268$, $B = 0$, $D = -17/30$.

6. Numerical solutions of the initial value problem

We conclude by considering the dynamics of the system on 2π -periodic domains, i.e. we solve numerically the problem:

$$\eta_\tau + (\eta u)_x = 0 \quad (37)$$

$$(u_\tau + uu_x) + \beta \eta_x = W_e \eta_{xxx}, \quad (38)$$

with initial conditions given by

$$\eta(x, 0) = 1 + 0.3 \cos(x), \quad u(x, 0) = 0.3 \sin(x). \quad (39)$$

Conditions (39) are chosen to preserve certain symmetries in the solutions, but the phenomena described next arise for more general conditions also. Adaptive spectral methods are used to compute the dynamics to large times or until there is a singular event as described next (see for example [10]). Two canonical cases are computed in order to present the generic phenomena supported by the equations. The Weber number is taken to be $W_e = 1/2$ and in the first case we take $\beta = -1$ while in the second $\beta = 1$. These choices are motivated by the linear theory of Section 3 and correspond to a weak and strong electric field, respectively, as can be seen from the definition $\beta = E_b(1 - \epsilon_p)^2 - (\rho - 1)$. When $\beta = -1$ the linear Rayleigh–Taylor (R–T) instability is operational (we take $\rho = 2$ for definiteness, in all computations) whereas as E_b increases to yield $\beta = 1$ we obtain a linear stabilization of R–T. The results of Fig. 4 follow the dynamics into the nonlinear regime. Panels (a)–(c) correspond to $\beta = -1$ while panel (d) corresponds to $\beta = 1$. In the former case the electric field is not strong enough to suppress R–T and η_{\min} is seen to reach zero in finite time, with the flow terminating in a finite time singularity (see panel (a)). The finite time touchdown is evident in panel (b) which follows the spatiotemporal evolution of $\eta(x, t)$ and interestingly the emerging touchdown shape consists of large drops separated by smaller satellite drops, a nonlinear phenomenon observed in other similar contexts also (see for example the recent review paper by Craster and Matar [3]). The horizontal velocity u blows up as the singular time is approached and this is clearly seen in panel (c) where large fluid velocities are found in the vicinity of the touchdown points. When E_b is increased sufficiently so that $\beta = 1$, the R–T instability is suppressed and the system undergoes nonlinear oscillations in time which are in fact quasi-periodic (this has been confirmed by constructing Poincaré maps – not shown). More

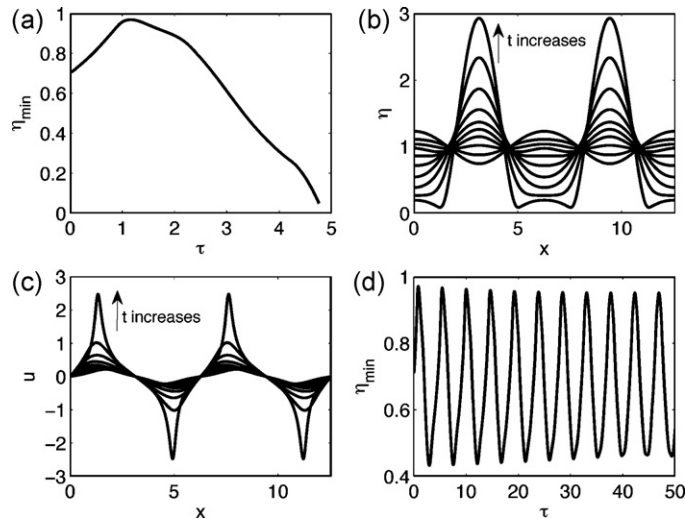


Fig. 4. (a) Evolution of η_{\min} showing touchdown of the lower wall for the case $W_e = 0.5$ and $\beta = -1$. (b) Corresponding evolution of $\eta(x, \tau)$. Interface η is captured with time interval 0.5 units at $\tau = 0.2, 0.7, \dots, 4.7$. (c) Corresponding evolution of the horizontal velocity $u(x, \tau)$. (d) Evolution of η_{\min} in the stable regime with $\beta = 1$ and $W_e = 0.5$.

detailed numerics and analysis is needed to classify the singular solutions, but preliminary work indicates that the structures are self-similar.

7. Discussion

This study shows theoretically and numerically that Rayleigh–Taylor instability can be removed by imposing a sufficiently strong electric field, even in the absence of surface tension. Inviscid flows have been considered and the fluids are taken to be perfect dielectrics. The asymptotic limit of a thin upper layer has been studied in detail and a system of coupled evolution equations for the interfacial shape and the corresponding horizontal velocity, have been derived. These equations support periodic traveling waves and also solitary waves. The stability of these waves is left for a future investigation. Numerical solutions of the initial value problem on periodic domains show that when Rayleigh–Taylor instability is active the model predicts wall touchdown in finite time; this can be suppressed by a strong enough electric field and our numerical work indicates that the system evolves to time oscillatory nonlinear motions in such cases.

Acknowledgements

The work of LLB was partly supported by the University Research Council Seed Grant, University of Idaho. The work of DTP and PGP was partly supported by the National Science Foundation grant DMS-0072228.

References

- [1] G. Baker, R. Caflisch, M. Siegel, Singularity formation during Rayleigh–Taylor instability, *J. Fluid Mech.* 252 (5) (1993) 51–78.
- [2] I. Bronshtein, K. Semendiyev, G. Musiol, H. Muehlig, *Handbook of Mathematics*, 4th ed. edition, Springer, 2004.
- [3] R.V. Craster, O.K. Matar, Dynamics and stability of thin liquid films, *Rev. Mod. Phys.* 81 (2009) 1131–1198.
- [4] H. Gleeson, P. Hammerton, D.T. Papageorgiou, J.M. Vanden-Broeck, A new application of the Korteweg–de Vries Benjamin–Ono equation in interfacial electrohydrodynamics, *Phys. Fluids* 19 (3) (2007) 031703.
- [5] S. Grandison, D.T. Papageorgiou, J.-M. Vanden-Broeck, Interfacial capillary waves in the presence of electric fields, *Eur. J. Mech. B Fluids* 26 (3) (2007) 404–421.
- [6] S. Grandison, D.T. Papageorgiou, J.-M. Vanden-Broeck, The influence of electric fields and surface tension on Kelvin–Helmholtz instability in two-dimensional jets, *ZAMP* (submitted for publication).
- [7] J.D. Jackson, *Classical Electrodynamics*, Wiley, New York, 1999.

- [8] J.R. Melcher, W.J. Schwarz, Interfacial relaxation overstability in a tangential electric field, *Phys. Fluids* 11 (12) (1968) 2604–2616.
- [9] D.T. Papageorgiou, J.-M. Vanden-Broeck, Large-amplitude capillary waves in electrified fluid sheets, *J. Fluid Mech.* 508 (2004) 71–88.
- [10] B.S. Tilley, P.G. Petropoulos, D.T. Papageorgiou, Dynamics and rupture of planar electrified liquid sheets, *Phys. Fluids* 13 (12) (2001) 3547–3563.
- [11] D. Tseluiko, D.T. Papageorgiou, A global attracting set for nonlocal Kuramoto–Sivashinsky equations arising in interfacial electrohydrodynamics, *Eur. J. Appl. Math.* 17 (6) (2006) 677–703.
- [12] D. Tseluiko, D.T. Papageorgiou, Wave evolution on electrified falling films, *J. Fluid Mech.* 556 (2006) 361–386.
- [13] D. Tseluiko, D.T. Papageorgiou, Nonlinear dynamics of electrified thin liquid films, *SIAM J. Appl. Math.* 67 (5) (2007) 1310–1329 (electronic).